



Influence of Pb and Co-doping on photocatalytic degradation performance of ZnO thin films

Fatemeh Moosavi^{*1}, Mohammad Ebrahim Bahrololoom¹, Ramin Kamjou²

¹Department of Materials Science and Engineering, School of Engineering, Shiraz University, Shiraz, Iran;

²Jahrom Organization of Education, Jahrom, Iran.

Received: 16 May 2021; Accepted: 28 August 2021

*Corresponding author email: fateme.moosavi68@gmail.com

ABSTRACT

Nanostructured ZnO thin films with two different dopants namely Pb and Co were prepared by a sol-gel method. The thin films have been prepared from zinc acetate, monoethanolamine and iso-propanol and then they were deposited on glass substrate by using a dip coating method. The structural, morphological, photocatalytic activity and optical absorbance of thin films were investigated by X-ray diffraction (XRD), scanning electron microscopy (SEM), ultraviolet-visible spectrophotometer and degradation of methylene blue dye (MB). The all thin films exhibited a polycrystalline hexagonal wurtzite structure that revealed by XRD. Due to doping, the average grain size of ZnO thin film increased. All films showed a wrinkle morphology. Photocatalytic activity of thin films was evaluated in aqueous solutions of Methylene Blue (MB) under UV-light illumination. The results indicated that the photocatalytic activity of ZnO thin films increased by Pb doping, conversely Co doping reduced the photocatalytic activity in comparison with the pure ZnO films. Hence speed of degradation of methylene blue by Pb doped ZnO is higher than that of pure and Co doped ZnO.

Keywords: Co-doping, Pb-doping, Photocatalyst, Sol-Gel, ZnO

1. INTRODUCTION

ZnO is a II-VI semiconductor with hexagonal wurtzite structure that has wide band gap (3.37 eV) and large exciton binding energy (60 meV) [1, 2]. Doping of ZnO with metal elements leads to many attractive properties [3, 4]. Therefore, ZnO is suitable for many applications such as dye sensitized solar cells [5], electro optic applications [6], UV lasers [7], field effect transistors [8], UV detectors [9], gas sensor [10], surface enhanced Raman spectroscopy [11] and photocatalysts [12]. The shape, size, impurities, doping level and type, and present phases are the key factors affecting on the properties of ZnO.

The photocatalysts have been applied and developed for the removal of dyes from industrial effluents [13, 14]. ZnO and TiO₂ are two of the most important of environmental photocatalysts with semiconducting properties [15]. Even though photocorrosion often occurs with the lighting of UV light in the case of ZnO in aqueous solution that reduces photocatalytic activity [16, 17], some studies have approved that ZnO even in aqueous solution, has a good photocatalytic activity for some dyes [18, 19]. Due to large exciton binding energy, superior physical, non-toxicity, low cost and chemical stability [20, 21], attention to this nanostructure has increased in the recent years and

many researchers have focused on the synthesis of doped and undoped nanostructures that zinc oxide is one of the most important of them [22]. Doped ZnO nanostructures has applied in optoelectronics[23], spin valves, spin light emitting diodes, magnetic sensors, non-volatile memory devices[24, 25] and photocatalysis[26].

So far, zinc oxide thin films have been applied by various methods such as sputtering[27], chemical vapor deposition[28], sol-gel[29], pulsed laser deposition[30] and others. Among these methods, sol gel method is common and popular method due to its simplicity, low synthesis temperature and high purity of the resultant products [31]. In this work, Pb- and Co-doped ZnO thin films were coated on glass substrates by sol gel method for first time and the influence of doping on microstructure, morphology, optical properties and photocatalytic activity was investigated.

2. EXPERIMENTAL

2.1. Synthesis

Zinc oxide thin films doped with Pb and Co, were deposited on the glass slides by a sol-gel dip coating method. The solution was prepared by dissolving 0.3M zinc acetate dehydrate ($\text{Zn}(\text{CH}_3\text{COO})_2 \cdot 2\text{H}_2\text{O}$) in 10 ml iso-propanol ($\text{CH}_3\text{C}_2\text{H}_5\text{OH}$) containing monoethanolamin (as a stabilizer) in which mole ratio of Zn^{2+} to MEA was kept to 1:1. The required amounts of lead acetate trihydrate ($\text{Pb}(\text{CH}_3\text{COO})_2 \cdot 3\text{H}_2\text{O}$) and cobalt acetate tetrahydrate ($\text{Co}(\text{CH}_3\text{COO})_2 \cdot 4\text{H}_2\text{O}$) were separately dissolved in two above solution to obtain solution of Pb- and Co- doped ZnO (mole ratio of Pb^{2+} and Co^{2+} to $\text{Zn}^{2+}=0.1$). The obtained solutions were stirred at 70°C for 1 h. Then, a clear and homogeneous solutions was obtained and after aging for 1 day it was used as the coating solution by the sol-gel dip coating. Final thin films (Pb doped ZnO and Co doped ZnO) were deposited on glass substrates (10 mm × 15 mm × 1.5 mm) at room temperature. The glass substrates were dipped in the precursor solutions for 2 min. The layers were deposited for 10 times coating and dried in an oven at 80°C after each successive coating to remove the solvent. The gel films were annealed at 400°C for 1 h and then, the thin films were cooled to room temperature to obtain the pure, Pb and Co-doped ZnO thin films.

2.2. Characterization

The crystal structure of the un-doped, Pb

and Co-doped ZnO thin films was identified by an X-ray diffractometer (XRD, D-8 Advanced). Surface morphology of the thin films were imaged by scanning electron microscopy (SEM, S-360 Cambridge), acted at 20 kV acceleration voltage. UV-Vis absorbance spectra of thin films were obtained by Ultraviolet-visible spectrophotometer (UV-4802UNCO) at room temperature.

2.3. Photocatalytic degradation

The photocatalytic activities of thin films were evaluated by means of the degradation of methylene blue (MB) in an aqueous solution under the UV light irradiation. The degradation reaction was performed in a glass container containing MB solution at an initial concentration of 10 mg/lit (10 ppm). Then, the thin films were immersed in the glass container containing 20 mL of MB solution and the thin films were irradiated with two parallel UV lamps in a dark space (two 8-watt mercury lamps made by Philips). The lamps were fixed at a distance of approximately 10 cm from the prepared solution. To investigate the possible reaction between the photocatalyst and methylene blue, the samples were first placed in a darkness for 45 minutes. The concentration of residual MB after irradiating for 0.5, 1, 1.5, 2, 2.5 and 3 h, was determined by the same UV-Vis spectrophotometer used for measurement of the optical transmission spectra of the thin films. The degradation efficiency was determined from the following equation [32]:

$$D = \left[\frac{C_0 - C}{C_0} \right] \times 100 \quad (1)$$

Where D is degradation efficiency, C_0 and C are initial concentration of dye and concentration of dye after irradiation, respectively.

3. RESULTS AND DISCUSSION

3.1. XRD analysis

The XRD patterns of the undoped ZnO, Pb doped ZnO and Co doped ZnO thin films are shown in Fig. 1(a-c), respectively. The XRD peaks for (100), (200) and (101) planes indicate that all the films have a polycrystalline hexagonal wurtzite structure (JCPDS card no. 36-1451). The diffraction peaks of lead oxide (PbO) and cobalt oxide (Co_3O_4) were identified in the XRD patterns of Pb doped ZnO and Co doped ZnO thin films. The doped Pb and Co in ZnO is more than the solubility limit of Pb and Co in ZnO matrix. It can increase effectively

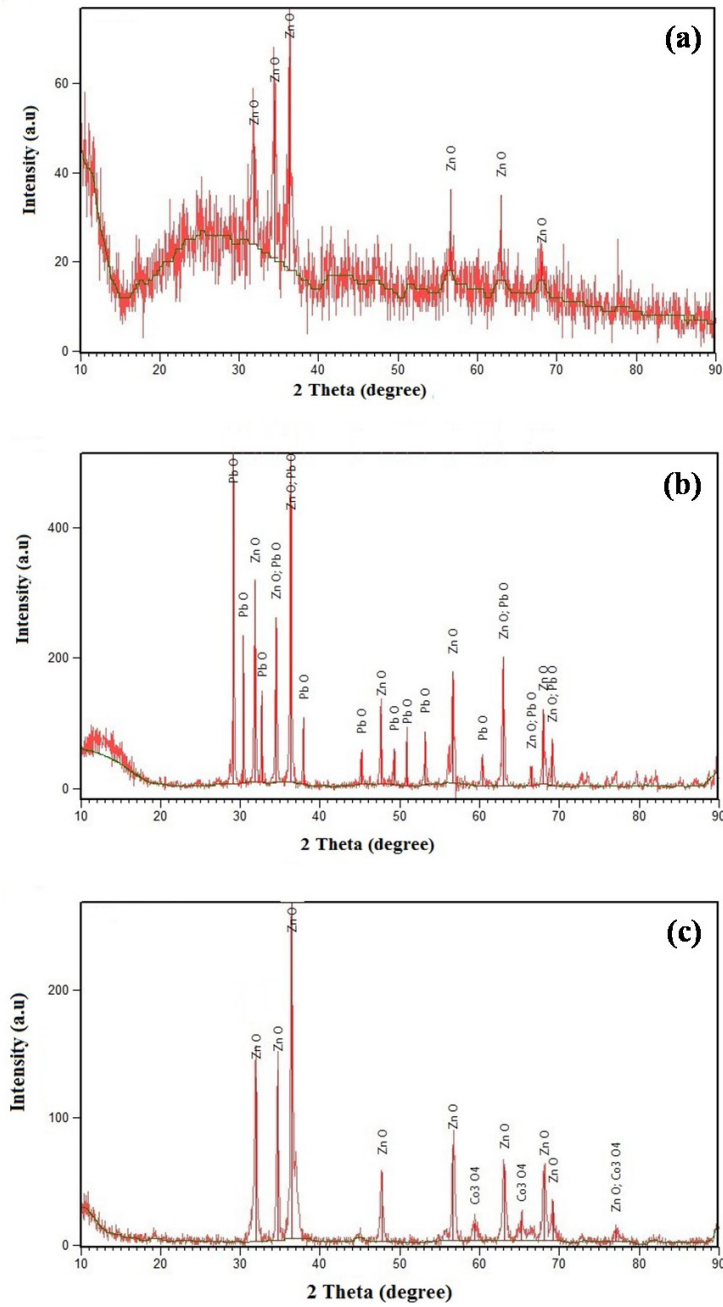


Fig. 1- XRD patterns of (a) ZnO (b) Pb-doped ZnO and (c) Co-doped ZnO thin films.

the possibility of secondary impurity. Pb and Co doping shifted the XRD peaks to higher angles. The same results were also report by Ahmad et.al for Pb doping[33] and Nair et.al for Co doping[34].

The average crystallite size was estimated by using of Scherrer's equation[35]:

$$d = \frac{k\lambda}{\beta \cos\theta} \quad (2)$$

Where k is a constant (0.9) and d, λ, θ are the average crystallite size (nm), wavelength of X-ray radiation (0.15406 nm) and Bragg's angle of diffraction respectively and β is full-width at half maximum intensity of the most intense peak. Pb and Co doping increased the average crystallite size from 21.245 nm to 27.86 nm and 34 nm, respectively. Therefore, it can be concluded

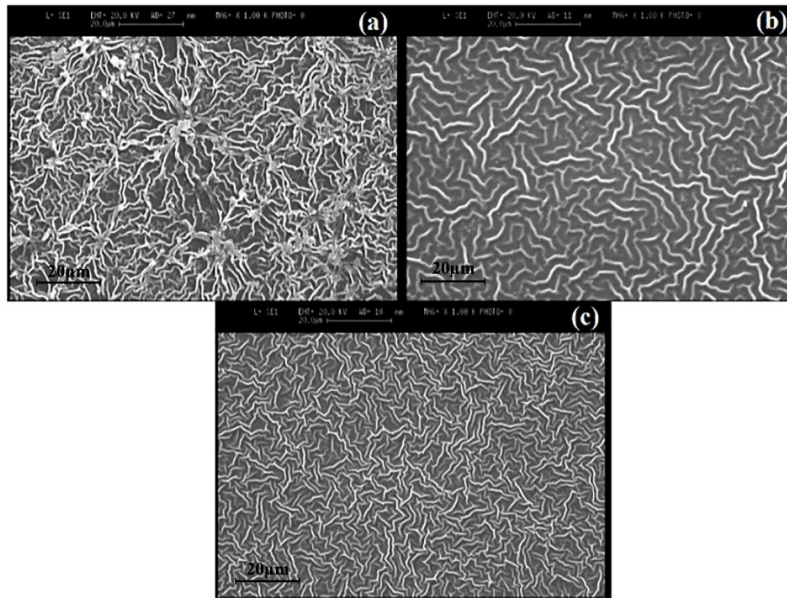


Fig. 2- SEM micrographs of (a) ZnO thin film, (b) Pb-doped ZnO thin film and (c) Co-doped ZnO.

that all thin films are nanocrystalline in nature.

Using the Williamson-Hall method, the micro-strain on the thin film nanostructures was analyzed. The Williamson-Hall equation can be shown as follows [36]:

$$\frac{\beta \cos \theta}{\lambda} = \frac{1}{D_{hkl}} + \epsilon_{hkl} \frac{\sin \theta}{\lambda} \quad (3)$$

Where θ is the diffraction angle, β is full-width at half maximum intensity of the peaks, λ is wavelength of X-ray radiation (0.15406 nm), D_{hkl} is crystallite size and ϵ_{hkl} is micro-strain. The micro-strain obtained for the samples was obtained as -0.000291 and -0.00146 for Pb doped and Co-doped samples, respectively. Negative values indicate compressive strain in ZnO lattice.

3.2. SEM analysis

The surface morphology of pure ZnO, and doped thin films are shown in Figure 2. It was observed that the pure ZnO thin film had a wrinkle morphology with an approximate width of 0.5-2 μm (Figure 2, a). Although Pb- and Co-doped ZnO thin films had the wrinkle morphology but doping has changed the shape and size of wrinkles (Figure 2, b and c). The width of wrinkles decreased to 0.8-1.2 μm and 0.4-0.8 μm for Pb- and Co doped thin films, respectively. The size of wrinkles in Co doped ZnO thin film were smaller than Pb doped ZnO thin film. The morphology of ZnO thin film

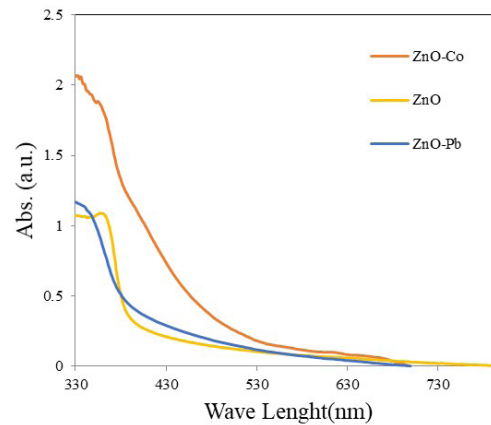


Fig. 3- UV-Vis absorbance spectra of undoped, Pb and Co doped ZnO thin films.

was not homogenous, while the morphology of Pb and Co doped thin films was homogenous.

3.3. Optical analysis

The optical absorbance spectra of pure, Pb and Co doped ZnO thin films deposited on glass substrates shown in Figure 3. The position of absorption spectra of ZnO thin films has been moved toward longer wavelength by Co doping and to lower wavelength by Pb doping. It occurs due to increase in the band gap with doping. Burstein-Moss effect can be explained the increase in the band gap or blue shift [37]. The Fermi level combine in to the conduction band in this

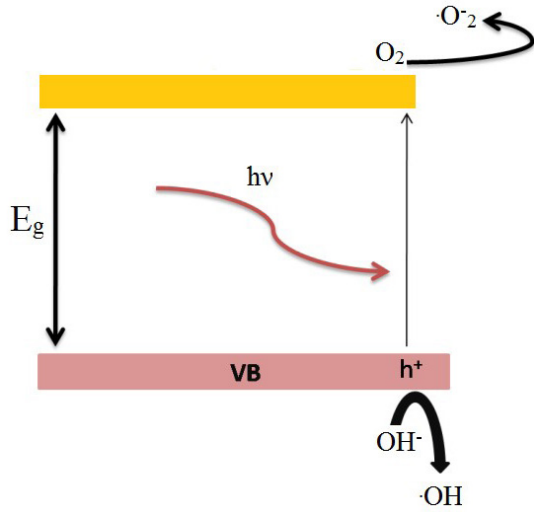
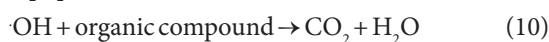
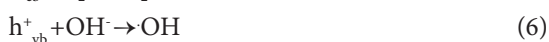


Fig. 4- Schematic mechanism of doped ZnO photocatalyst.

phenomenon[38]. Co doping has greater influence on band gap.

3.4. Photocatalytic activity

The photocatalytic activity of pure, Pb-and Co-doped ZnO thin films were investigated by degradation of methylene blue dye (MB) in an aqueous solution. The photocatalytic activity of ZnO thin films can be shown according to the following reactions[39]:



Where h_{vb}^+ is the electron vacancy and e_{cb}^- is the electron in conduction band. This mechanism is summarized in Figure 4.

Figure 5 shows the degradation curves of methylene blue (%) versus time for pure, Pb-and Co-doped ZnO. It is observed from this figure that Pb-doping has increased the photocatalytic activity. Because of the increase in band gap energy of Pb-doped ZnO, stability of excitons increase, therefore photocatalytic activity of ZnO thin films were increased. Co-doping decreased the photocatalytic activity of ZnO thin film. In fact, Co doped ZnO cannot significantly degrade MB

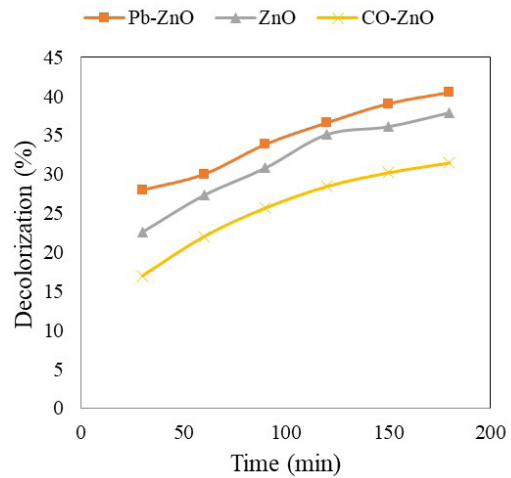


Fig. 5- Time dependence of the de-colorization efficiency of MB solution by doped and undoped ZnO thin films.

due to the formation of a new phase. Moreover, agglomeration of Co on the surface of Co-doped ZnO thin films decreases the effective surface active sites and accordingly photocatalytic activity decreased [40]. In fact, it can be said that in the same time, doped thin film with Pb decomposes more methylene blue.

4. CONCLUSIONS

Pure ZnO as well as Pb-and Co-doped ZnO thin films were prepared by a sol-gel method. The structure, morphology, optical and photocatalytic properties of ZnO, Pb and Co doped ZnO nanostructures were investigated. The results showed that thin films had nanostructure nature with hexagonal wurtzite structure. It was observed that absorbance edge of ZnO thin film was shifted to higher and lower wavelengths by Co-doping and Pb-doping, respectively. The photocatalytic activity of thin films was investigated by decomposition of MP under UV light illumination. Photocatalytic activity of ZnO thin films was increased and decreased by Pb-doping and Co-doping, respectively. Therefore, Pb doping can improve the photocatalytic activity in UV range and Co-doping ZnO thin film can be used as photocatalyst in visible light wavelength range.

References

1. Ma L, Ai X, Huang X, Ma S. Effects of the substrate and oxygen partial pressure on the microstructures and optical properties of Ti-doped ZnO thin films. *Superlattices and Microstructures*. 2011;50(6):703-12.
2. Sankara Reddy B, Venkatramana Reddy S, Koteeswara Reddy N, Prabhakara Reddy Y. Structural, Optical And Magnetic Prop-

- erties Of (Fe, Ag) Co-doped ZnO Nanostructures. *Advanced Materials Letters*. 2014;5(4):199-205.
3. Moosavi F, Bahrololoom ME, Kamjou RA. Effects of Cu doping on nano structure, morphology and photocatalytic activity of ZnO thin film synthesized by sol-gel method. *Stud. UBB Chem*. 2016 Mar 1;1:79.
 4. Li Z, Zhang G, Gao W, Zhao R, Wang Y. Ag decorated ZnO nanocrystallines synthesized by a low-temperature solvothermal method and their application for high response H₂ gas sensor. *Journal of Materials Science: Materials in Electronics*. 2019;30(20):18959-69.
 5. Zhang Q, Dandeneau CS, Zhou X, Cao G. ZnO Nanostructures for Dye-Sensitized Solar Cells. *Advanced Materials*. 2009;21(41):4087-108.
 6. Shi D, Guo Z, Bedford N. Electro-Optical and Piezoelectric Applications of Zinc Oxide. *Nanomaterials and Devices: Elsevier*; 2015. p. 175-90.
 7. da Silva-Neto ML, de Oliveira MCA, Dominguez CT, Lins REM, Rakov N, de Araújo CB, et al. UV random laser emission from flexible ZnO-Ag-enriched electrospun cellulose acetate fiber matrix. *Scientific reports*. 2019;9(1):11765-.
 8. Dahiya AS, Opoku C, Oshman C, Poulin-Vittrant G, Cayrel F, Tran Huu Hue LP, et al. Zinc oxide sheet field-effect transistors. *Applied Physics Letters*. 2015;107(3):033105.
 9. Khokhra R, Bharti B, Lee H-N, Kumar R. Visible and UV photo-detection in ZnO nanostructured thin films via simple tuning of solution method. *Scientific reports*. 2017;7(1):15032-.
 10. Aroutiounian VM. Zinc Oxide Gas Sensors. *Journal of Contemporary Physics (Armenian Academy of Sciences)*. 2020;55(4):323-33.
 11. Chou C-M, Thanh Thi LT, Quynh Nhu NT, Liao S-Y, Fu Y-Z, Hung LVT, et al. Zinc Oxide Nanorod Surface-Enhanced Raman Scattering Substrates without and with Gold Nanoparticles Fabricated through Pulsed-Laser-Induced Photolysis. *Applied Sciences*. 2020;10(14):5015.
 12. Kuriakose S, Satpati B, Mohapatra S. Enhanced photocatalytic activity of Co doped ZnO nanodisks and nanorods prepared by a facile wet chemical method. *Physical Chemistry Chemical Physics*. 2014;16(25):12741.
 13. Gelover S, Mondragón P, Jiménez A. Titanium dioxide sol-gel deposited over glass and its application as a photocatalyst for water decontamination. *Journal of Photochemistry and Photobiology A: Chemistry*. 2004;165(1-3):241-6.
 14. Yun J, Jin D, Lee Y-S, Kim H-I. Photocatalytic treatment of acidic waste water by electrospun composite nanofibers of pH-sensitive hydrogel and TiO₂. *Materials Letters*. 2010;64(22):2431-4.
 15. Hariharan C. Photocatalytic degradation of organic contaminants in water by ZnO nanoparticles: Revisited. *Applied Catalysis A: General*. 2006;304:55-61.
 16. Neppolian B, Sakthivel S, Arabindoo B, Palanichamy M, Murugesan V. Degradation of textile dye by solar light using TiO₂ and ZnO photocatalysts. *Journal of Environmental Science and Health, Part A*. 1999;34(9):1829-38.
 17. van Dijken A, Janssen AH, Smitsmans MHP, Vanmaekelbergh D, Meijerink A. Size-Selective Photoetching of Nanocrystalline Semiconductor Particles. *Chemistry of Materials*. 1998;10(11):3513-22.
 18. Dindar B, Içli S. Unusual photoreactivity of zinc oxide irradiated by concentrated sunlight. *Journal of Photochemistry and Photobiology A: Chemistry*. 2001;140(3):263-8.
 19. Gouvêa CAK, Wypych F, Moraes SG, Durán N, Nagata N, Peralta-Zamora P. Semiconductor-assisted photocatalytic degradation of reactive dyes in aqueous solution. *Chemosphere*. 2000;40(4):433-40.
 20. Etacheri V, Roshan R, Kumar V. Mg-Doped ZnO Nanoparticles for Efficient Sunlight-Driven Photocatalysis. *ACS Applied Materials & Interfaces*. 2012;4(5):2717-25.
 21. Welderfael T, Yadav OP, Tadesse AM, Kaushal J. Synthesis, characterization and photocatalytic activities of Ag-N-codoped ZnO nanoparticles for degradation of methyl red. *Bulletin of the Chemical Society of Ethiopia*. 2013;27(2).
 22. Yousefi R, Jamali-Sheini F, Sa'edi A, Zak AK, Cheraghizade M, Pilban-Jahromi S, et al. Influence of lead concentration on morphology and optical properties of Pb-doped ZnO nanowires. *Ceramics International*. 2013;39(8):9115-9.
 23. Panigrahy B, Aslam M, Bahadur D. Aqueous Synthesis of Mn- and Co-Doped ZnO Nanorods. *The Journal of Physical Chemistry C*. 2010;114(27):11758-63.
 24. Balti I, Mezni A, Dakhlaoui-Omrani A, Léone P, Viana B, Brinza O, et al. Comparative Study of Ni- and Co-Substituted ZnO Nanoparticles: Synthesis, Optical, and Magnetic Properties. *The Journal of Physical Chemistry C*. 2011;115(32):15758-66.
 25. Pearton SJ, Abernathy CR, Norton DP, Hebard AF, Park YD, Boatner LA, et al. Advances in wide bandgap materials for semiconductor spintronics. *Materials Science and Engineering: R: Reports*. 2003;40(4):137-68.
 26. Barakat MA, Schaeffer H, Hayes G, Ismat-Shah S. Photocatalytic degradation of 2-chlorophenol by Co-doped TiO₂ nanoparticles. *Applied Catalysis B: Environmental*. 2005;57(1):23-30.
 27. Park TE, Kong BH, Cho HK, Park DJ, Lee JY. Influence of gas atmosphere during growth interruption in the deposition of ZnO films by magnetron sputtering. *Physica B: Condensed Matter*. 2006;376-377:735-40.
 28. Deng H, Russell JJ, Lamb RN, Jiang B, Li Y, Zhou XY. Microstructure control of ZnO thin films prepared by single source chemical vapor deposition. *Thin Solid Films*. 2004;458(1-2):43-6.
 29. Peng F, Wang H, Yu H, Chen S. Preparation of aluminum foil-supported nano-sized ZnO thin films and its photocatalytic degradation to phenol under visible light irradiation. *Materials Research Bulletin*. 2006;41(11):2123-9.
 30. Lemlikchi S, Abdelli-Messaci S, Lafane S, Kerdja T, Guitoum A, Saad M. Study of structural and optical properties of ZnO films grown by pulsed laser deposition. *Applied Surface Science*. 2010;256(18):5650-5.
 31. Pal B, Sharon M. Enhanced photocatalytic activity of highly porous ZnO thin films prepared by sol-gel process. *Materials Chemistry and Physics*. 2002;76(1):82-7.
 32. Kaneva NV, Dimitrov DT, Dushkin CD. Effect of nickel doping on the photocatalytic activity of ZnO thin films under UV and visible light. *Applied Surface Science*. 2011;257(18):8113-20.
 33. Ahmad M, Pan C, Yan W, Zhu J. Effect of Pb-doping on the morphology, structural and optical properties of ZnO nanowires synthesized via modified thermal evaporation. *Materials Science and Engineering: B*. 2010;174(1-3):55-8.
 34. Nair MG, Nirmala M, Rekha K, Anukaliani A. Structural, optical, photo catalytic and antibacterial activity of ZnO and Co doped ZnO nanoparticles. *Materials Letters*. 2011;65(12):1797-800.
 35. Thongsuriwong K, Amornpitoksuk P, Suwanboon S. Structure, morphology, photocatalytic and antibacterial activities of ZnO thin films prepared by sol-gel dip-coating method. *Advanced Powder Technology*. 2013;24(1):275-80.
 36. Parchur AK, Ansari AA, Singh BP, Hasan TN, Syed NA, Rai SB, et al. Enhanced luminescence of CaMoO₄:Eu by core@shell formation and its hyperthermia study after hybrid formation with Fe₃O₄: cytotoxicity assessment on human liver cancer cells and mesenchymal stem cells. *Integr Biol*. 2014;6(1):53-64.

37. Yang H, Nie S. Preparation and characterization of Co-doped ZnO nanomaterials. *Materials Chemistry and Physics*. 2009;114(1):279-82.
38. Sakai K, Kakeno T, Ikari T, Shirakata S, Sakemi T, Awai K, et al. Defect centers and optical absorption edge of degenerated semiconductor ZnO thin films grown by a reactive plasma deposition by means of piezoelectric photothermal spectroscopy. *Journal of Applied Physics*. 2006;99(4):043508.
39. Jongnavakit P, Amornpitoksuk P, Suwanboon S, Ndiege N. Preparation and photocatalytic activity of Cu-doped ZnO thin films prepared by the sol-gel method. *Applied Surface Science*. 2012;258(20):8192-8.
40. Lu Y, Lin Y, Wang D, Wang L, Xie T, Jiang T. A high performance cobalt-doped ZnO visible light photocatalyst and its photogenerated charge transfer properties. *Nano Research*. 2011;4(11):1144-52.